

Forensic Injury Biomechanics

Wilson C. Hayes, Mark S. Erickson,
and Erik D. Power

Hayes+Associates, Inc., Corvallis, Oregon 97333; email: wch@hayesassoc.com

Annu. Rev. Biomed. Eng. 2007. 9:55–86

First published online as a Review in Advance on
April 20, 2007

The *Annual Review of Biomedical Engineering* is
online at bioeng.annualreviews.org

This article's doi:
[10.1146/annurev.bioeng.9.060906.151946](https://doi.org/10.1146/annurev.bioeng.9.060906.151946)

Copyright © 2007 by Annual Reviews.
All rights reserved

1523-9829/07/0815-0055\$20.00

Key Words

injury criteria, motor vehicle collisions, slips, falls, recreational activities

Abstract

Forensic injury biomechanics is the science that relates mechanical forces to disruption of anatomical regions of the human body. In this review, we introduce (*a*) how scaling techniques can be used to describe injury severity and probability of death; (*b*) how a simple ratio, the factor of risk, and more sophisticated injury risk functions can be used to determine the probability of injury; and (*c*) how injury criteria (also known as tolerance limits) are defined for the head and neck. Methods for establishing injury causation are then illustrated by real-world examples drawn from litigation involving motor vehicle collisions and slips, trips and falls. Those factors that distinguish litigation from basic and applied research are also discussed, including the criteria for admissibility of expert opinions and the level of certainty used as the basis for these opinions. The criteria that must be met to support opinions on causation at both epidemiological and individual levels are also noted. If the expert appreciates the difference between the demands of litigation and those of basic and applied research, expert opinion can play a crucial role in the decision-making process that characterizes litigation. Because forensic injury biomechanics is central to opinions on injury causation, and because causation is often the key to determinations of who is at fault, forensic injury biomechanics can be the deciding factor in many personal injury, products and premises liability, wrongful death, and criminal cases.

Contents

INTRODUCTION.....	56
Expert Opinion in Litigation.....	57
INJURY RISK PREDICTION.....	58
Injury Scaling.....	58
Factor of Risk.....	60
Injury Risk Functions.....	61
INJURY CRITERIA.....	62
Head.....	62
Neck Injury Criteria.....	65
APPLICATIONS.....	68
Motor Vehicle Collisions.....	68
Slips, Trips, and Falls.....	73
SUMMARY.....	80

INTRODUCTION

A father is killed by a drunk driver in a high speed T-bone collision as he executes a legal U-turn to pick up his ten-year-old daughter. She is a horrified witness to the event. An office worker claims that she slipped on a linoleum floor, falling forward and fracturing her knee cap. A resident of a long-term care facility, prone to seizures from an earlier traumatic brain injury, falls to his death from a third-story balcony. Did he fall or jump? An adult male slips and falls backward, resulting in a fracture/dislocation of his cervical spine after only two low-height bounces on a backyard trampoline. The parties or their families are in court seeking compensation, with demands that sometimes seem to outstrip the claimed injuries or have little prospect of covering the costs of lifetime care or providing compensation for the loss of a loved one. How can a way be found through the often-conflicting stories and competing claims in cases involving personal injury, wrongful death, and criminal acts to arrive at an understanding of the mechanisms of injury and a determination of who was at fault?

The term forensic describes the application of scientific knowledge to legal problems. Defining injury as a failure of an anatomic structure and biomechanics (in the context of this chapter) as an application of mechanical engineering concepts to the human body, we define forensic injury biomechanics as the scientific field focused on how and if mechanical forces cause disruption to anatomic regions of the human body. What then is the scientific basis for determining if a particular event caused one or more injuries? In some cases, the injuries are obvious and not in dispute, for example, a fractured hip from a fall. In many cases, however, whether or not a traumatic event caused an injury is very much in dispute, for example, whether a herniated disc in the neck is a consequence of a low-speed rear-end collision or instead spinal arthritis associated with aging.

To address these questions, this review introduces (a) how scaling techniques can be used to describe injury severity and probability of death; (b) how a simple ratio, the factor of risk, and more sophisticated injury risk functions can be used to determine the probability of injury; and (c) how injury criteria are defined for the head and neck, anatomic sites that are important aspects of many cases involving forensic injury biomechanics. Methods for establishing injury causation are then illustrated by real-world examples drawn from litigation involving motor vehicle collisions; slips, trips, and falls; and occupational and recreational activities. Before describing the methods used in forensic injury biomechanics, factors that distinguish litigation from basic and applied research are noted. These include the criteria for admissibility of expert opinion, the level of certainty required as a basis for expert opinion, and the adversarial nature of the proceedings. Litigation offers multiple roles to the expert, along with many scientific, ethical, and personal challenges. If these are clearly understood and addressed, the effective expert can play a crucial role in the search for truth and in the decision-making process that characterizes litigation. In many cases, forensic injury biomechanics provides the objective evidence that can be the deciding factor in personal injury, products and premises liability, wrongful death, and criminal cases.

Expert Opinion in Litigation

According to the Federal Rules of Evidence 702, “If scientific, technical or other specialized knowledge will assist the trier of fact (the *jury* in a *jury trial*, or the *judge* in a *bench trial*) to understand the evidence or to determine a fact in issue, a witness qualified as an expert, by knowledge, skill, experience, training or education may testify thereto in the form of an opinion or otherwise.” The rules for admissibility of evidence from expert witnesses differ from those criteria that are typically applied in fundamental and academic research presentations and publications. Opinions expressed by expert witnesses must be based on reliable facts, data, and methodology (1). In most civil cases, the legal requirements for stating an expert opinion are the same as the burden of proof for civil cases, i.e., a “preponderance” of the evidence, “more likely than not,” or “at least 51%” (1). This is a lesser burden of proof than the “beyond a reasonable doubt” standard that applies in criminal cases. An expert opinion that is more probable than not (i.e., there is at least 51% probability) is also a far different standard than the $p < 0.05$ criterion that is used for making inferences from statistical comparisons in scientific research.

The facts, scientific principles, and methodologies relied on by experts as bases for their opinions must result in valid and reasonably accurate conclusions. Methodology relied on by experts can be challenged based on a series of legal decisions known as *Daubert* and their progeny. In rendering decisions on the admissibility of expert opinions, the judge acts as a “gate keeper” charged with excluding unreliable expert testimony (2). The landmark court decision *Daubert v. Merrell Dow Pharmaceuticals, Inc.* identified four factors necessary to meet the specialized knowledge requirement of Federal Rule 702, including (a) whether the methodology used by the expert can be, and has been, tested; (b) whether the theory or methodology has been subjected to peer-review and publication; (c) whether there is a known rate of error for the

method that is appropriate for the case; and (*d*) whether the methodology is accepted within a relevant scientific community. An additional factor, based on subsequent court decisions, is whether the expert's theory or methodology has been used outside litigation and prior to the case at hand. Using the above criteria, an expert's opinion may be challenged by opposing counsel at a *Daubert* hearing (1). If successful, the expert's testimony can be excluded at trial, with important consequences for the case and the expert's reputation.

INJURY RISK PREDICTION

An opinion as to whether an event causes one or more injuries is grounded first in what is meant by causation, second in how injuries can be characterized quantitatively, and third in how quantitative injury assessments can be related to the mechanical forces that produce them. With respect to causation, the classic work by Bradford-Hill (3) and others (4) has focused on criteria necessary to make inferences on causation from epidemiological (population-based) studies of disease. The Bradford-Hill criteria include an appropriate temporal sequence, i.e., that the health effect follows exposure, the specificity with which a risk factor is linked to a health outcome, the reversibility of the effect, the biological plausibility of the cause-effect relationships, the strength of the association between cause and effect, the consistency with which such cause-effect relationships are observed across multiple studies, and the slope of the dose-response gradient. However, court decisions usually involve individuals and not populations, and thus the population-based criteria to establish causation must be revised to apply to individuals. However, several of the epidemiological criteria for causation also apply to individuals. These include the requirement that the health effect (e.g., an injury) follow the exposure in an appropriate temporal sequence (i.e., not many months to years later or be pre-existing). There must be direct, objective evidence of both exposure and injury. Finally, the issue of biological plausibility can be replaced by one involving biomechanical plausibility. The issue of biomechanical plausibility means that, on a most fundamental level, when forces from an event imposed on an anatomic region are sufficiently high to exceed the strength or "tolerance limits" of that region, an event can be said to "cause" the injury. In the following sections, we first describe scaling procedures used to characterize the severity of injury and the probability of death from multiple injuries. We then describe biomechanical plausibility in more depth, first using a simple approach known as the factor of risk and then using more sophisticated, statistically based injury risk functions.

Injury Scaling

Injury scaling can be broadly defined as a means for quantitatively describing injuries. Anatomic injury scales, as expressed by the Abbreviated Injury Scale (AIS) and its extensions, are the scales most relevant to forensic injury biomechanics.

Abbreviated injury scale. The AIS was developed in the mid-1960s as a system to describe the severity of injuries throughout the body. The first AIS was published in

Table 1 The abbreviated injury score versus fatality rate (6)

Injury severity AIS	Severity code	Fatality rate (range %)
1	Minor	0.0
2	Moderate	0.1–0.4
3	Serious	0.8–2.1
4	Severe	7.9–10.6
5	Critical	53.1–58.4
6	Maximum (currently untreatable)	...

1971 and has since been revised in 1976, 1980, 1985, 1990, 1998, and 2005. The most recent update is referred to as AIS 2005. While the AIS was originally intended for traumatic injuries from motor vehicle collisions, the subsequent revisions now allow its application to a variety of injuries, including burns, gunshots, and falls (5). The AIS is an ordinal scale ranging from 1 (minor) to 6 (maximal–currently untreatable) (Table 1). The dictionary for AIS scaling is provided in the AIS Manual, organized into nine chapters, including (a) head (cranium and brain); (b) face; (c) neck; (d) thorax; (e) abdomen and pelvic contents; (f) spine (cervical, thoracic, and lumbar); (g) upper extremities; (h) lower extremities, pelvis, and buttocks; and (i) external (skin), thermal injuries, and other trauma. Within each chapter, detailed injury descriptions are provided for each specific anatomical component.

The AIS is a “threat to life” ranking, with higher AIS levels indicating an increased threat to life. The scores do not indicate relative magnitudes, e.g., an AIS level 3 injury is not three times as severe as an AIS 1 level injury. However, the larger the AIS value, the higher the corresponding rate of fatality (Table 1). This increase in fatality rate jumps rather markedly from AIS 3 to AIS 4 and even more dramatically from AIS 4 to AIS 5, with the former corresponding to a change from approximately 2% to approximately 10% and the latter from approximately 10% to more than 50% (7). This suggests that the forces that produce injuries that range between AIS 3 and AIS 4, and even more from AIS 4 to AIS 5, correspond to important regions of human tolerance, each representing a concomitant increase in fatality rates. AIS 2005 presents data on the correlation of the AIS severity scores with survival (8). Data from the National Trauma Data Base on 474,025 patients who sustained 1,291,191 injuries were analyzed. This is a data set of all patients who presented to trauma centers in the United States over the past several years. For a subset of 181,707 (38.3%) patients who sustained a single injury, survival risk ratios (SRRs) were determined for each injury in the AIS dictionary. These represent the number of patients who survived divided by the total number of patients who sustained the injury. Based on this definition, mortality equals 1–SRR. The data demonstrate that there is a strong nonlinear correlation between AIS severity and survival (as well as mortality) (see **Supplemental Figure 1**, follow the Supplemental Material link from the Annual Reviews home page at <http://www.annualreviews.org>). As shown, the data fit a quadratic function nearly perfectly. These data indicate that the AIS severity score performs extremely well as a measure of mortality, but mortality is not the sole determinant of AIS severity (8).

Injury severity score. The AIS is not designed to assess the combined effects of multiple injuries. There are two systems to do so, the Maximum AIS (MAIS) and the Injury Severity Score (ISS). The MAIS is simply the most severe (i.e., the highest level AIS code in a patient with multiple injuries). The MAIS is especially useful for comparing the frequency of specific injuries and their relative severity as well as changes in those frequencies from a vehicular design change (i.e., airbags) or a change in public policy (e.g., compulsory seatbelt use) (8). The ISS is widely used in trauma registries as a severity assessment tool. This scale is the sum of the squares of the highest AIS scores in three different body regions, including (a) head or neck, (b) face, (c) chest, (d) abdominal or pelvic content, (e) extremities or pelvic girdle, and (f) external. It is important to realize that the ISS body regions do not match the AIS chapters by body regions. In the ISS, the cervical spine is included in the neck, the thoracic spine is included in the chest, and the lumbar spine is included in the abdomen or pelvic contents. ISS scores range from 1 to 75, with a score of 75 corresponding to three AIS 5 injuries or to one AIS 6 injury. The ISS is given by

$$ISS = (AIS_1)^2 + (AIS_2)^2 + (AIS_3)^2, \quad (1)$$

where AIS_1 = highest AIS anywhere in the body, AIS_2 = highest AIS anywhere except body region of AIS_1 , and AIS_3 = highest AIS anywhere except body region of AIS_1 or AIS_2 .

Probability of death. As with the ISS, the probability of death (POD) makes use of AIS scaling but with several modifications (7). First, POD is calculated based on the two highest AIS values rather than three. Second, separate AIS values are assigned for soft tissue and for bony injuries. And third, the patient's age is taken into account. As described by Somers (9), the probability of death is given by

$$POD = e^X / (1 + e^X), \quad (2)$$

where $X = 2.2 (AIS_1) + 0.9 (AIS_2) - 11.25 + C$. Or, if age is available, $X = 2.7 (AIS_1) + 1.0 (AIS_2) + 0.06 \text{ age} - 15.4 + C$, and $C = -0.764$ for vehicles.

Factor of Risk

The simplest, and most intuitively obvious, approach to predicting injury risk makes use of the ratio between the loads imposed on an anatomic structure and the ultimate load-carrying capacity of that structure. This approach to injury risk prediction can be formalized by defining a factor of risk, Φ , as the ratio of the applied loads divided by the loads necessary to cause injury. This can be expressed as

$$\Phi = \text{Applied Force} / \text{Injury Force}. \quad (3)$$

This is the inverse of the factor of safety that is used widely by engineers to ensure that the force necessary to cause structural failure is well above the forces applied in service. Hayes et al. (10) used this approach in describing those factors that are important to age-related fractures of the hip. For a factor of risk exceeding one, injury to the anatomic region is likely. For a factor of risk well under one, fracture

is considered unlikely. For a skeletal structure such as the proximal femur, estimates of the factor of risk require information both on the forces to which the proximal femur is subjected and on the forces necessary to cause its fracture (10). Forces in both the numerator and denominator of Equation 3 should be for the same loading conditions. For instance, it would be inappropriate and inaccurate to compute a factor of risk for the neck by calculating Φ based on the forces applied to the neck under tension and extension loading conditions in the numerator and the forces necessary to cause fracture dislocation under compression/flexion loading conditions in the denominator. Use of a factor of risk is a powerful, intuitively satisfying and easily understood approach to injury risk prediction. Where the factor of risk is less compelling is in the region near $\Phi = 1$, where the approach suggests there should be a sharp transition between uninjured and injured. Because such an approach does not reflect the statistical variability inherent both in the applied loads and in the load-carrying capacities or tolerance limits of anatomic regions, more powerful approaches reflecting these statistical variabilities have been developed.

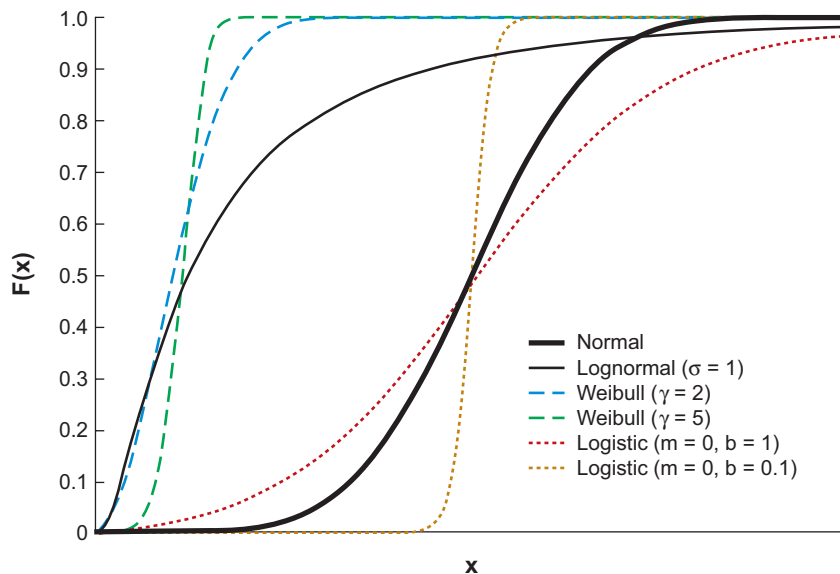
Injury Risk Functions

An approach that takes into account these statistical variabilities is the injury risk function. Such functions define relationships between the probability of injury and a particular parameter (e.g., subject age, mechanical load at an anatomic region). Laboratory experiments involving human cadavers are often performed to determine biomechanical response and injury tolerance level data. Several different statistical methods can then be used to generate injury risk functions based on these experimental data. The linear logistic model is commonly used to develop injury risk functions, primarily due to its ease of use. It has the form

$$p = \frac{1}{1 + e^{-\left(\alpha + \sum_{i=1}^n \beta_i \cdot x_i\right)}}, \quad (4)$$

where p is the probability, α is an intercept, and β_i are the coefficients associated with each independent predictor variable, x_i . Complete descriptions and the mathematical definitions of other distribution models can be found in statistical textbooks. Four of the more commonly applied models (Weibull, logistic, log-normal, and normal distributions) (**Figure 1**) were recently evaluated for appropriateness in modeling various injury datasets (11). No single distribution was found to be consistently more appropriate than any other for modeling the data, and the models differed appreciably only at the tails (risk of injury below 10% or above 90%) where the experimental data are sparse. Thus, it is typically unnecessary to evaluate the four different distributions when modeling an injury dataset because the statistical models equally well represent the biomechanical data. As would be expected, any estimation error associated with a statistical model is reduced as the total sample size is increased. Risk functions with a steeper shape have been found to require a smaller total number of samples to yield reliable results (12).

Figure 1
Shapes of various injury risk functions (11).



INJURY CRITERIA

Head

Given the potentially severe consequences of head and/or brain injury, the biomechanics research community has naturally maintained a longstanding focus on this anatomical region of the body.

Head injury criterion. Research toward the development of reliable injury measures for the head has been under way for more than 70 years (13). This early work produced the Wayne State Tolerance Curve (WSTC), which defined the boundary between safe and unsafe head acceleration levels (**Figure 2**). The WSTC was developed based on a series of head impact experiments using laboratory animals and human cadavers. The experiment protocols called for direct head impact with a rigid, flat impactor. Induced head accelerations were then measured with accelerometers placed diametrically opposite the impacted region. The head impact data demonstrated the fundamental notion that head injury is a function of linear head acceleration and impulse duration (14).

Based on the WSTC, later work by Gadd et al. (16) yielded a weighted impulse criteria used to predict brain injury. This criterion, known as the Gadd Severity Index (GSI), is a mathematical analog to the WSTC. One advantage of the GSI was that it eliminated the subjective visual comparison of a given head acceleration with the WSTC and replaced it with a quantifiable, mathematical injury metric. For a period of time, the GSI was adopted by the National Highway Traffic Safety Administration (NHTSA) and incorporated into Federal Motor Vehicle Safety Standard (FMVSS) 208. The criterion was used to evaluate how occupant restraints could mitigate against

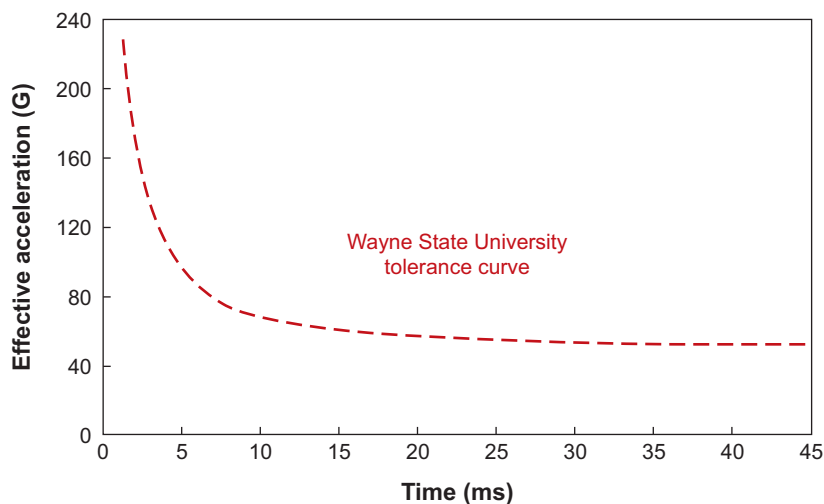


Figure 2

Area below curve considered safe. Area above curve associated with skull fracture and considered unsafe (15).

head injury (15). In the early 1970s, a modification of the GSI was proposed by Versace (17). This modification, a precursor to the currently used Head Injury Criterion (HIC), limited the time interval over which the GSI was evaluated. The current version of HIC is computed as (18)

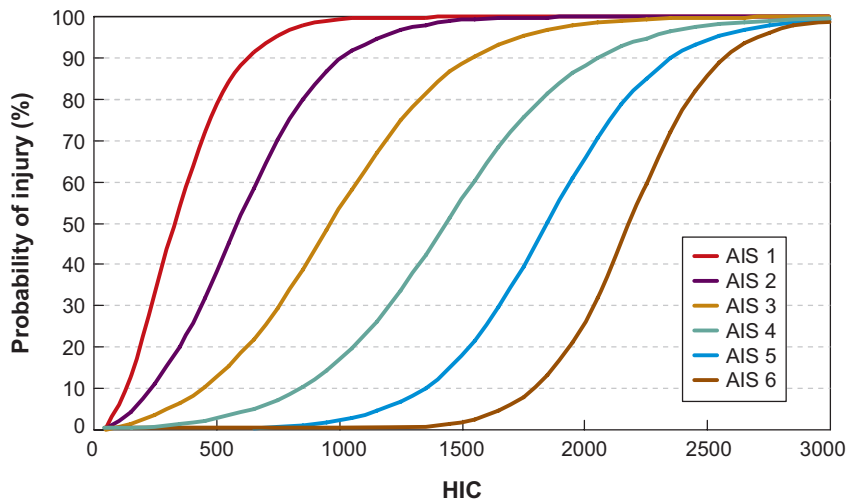
$$\text{HIC} = \max \left[\frac{1}{t_2 - t_1} \int_{t_1}^{t_2} a(t) dt \right]^{2.5} (t_2 - t_1), \quad (5)$$

where t_1 and t_2 are arbitrary times within the acceleration pulse. Acceleration, $a(t)$, is expressed as a multiple of gravitational acceleration ($g = 9.8 \text{ m/s}^2$; 32.2 ft/s^2). To pass FMVSS 208 successfully, automobile manufacturers must demonstrate, when subjected to a 30 mph frontal barrier impact, that a fully restrained 50th percentile male Anthropomorphic Test Device (ATD) is exposed to HIC scores of less than 700 and 1000, evaluated over maximum time intervals of 15 ms and 36 ms, respectively. HIC is currently the only head injury metric mandated by the NHTSA (19) to assess survivability of occupants in car crashes in the New Car Assessment Program (NCAP). Given its simple nature, along with its generally good correlation with experimental data, HIC is also used in forensic injury biomechanics.

Over the past several decades, HIC has been validated in many studies, under a variety of conditions. Using cadaver experiments, Prasad & Mertz (20) validated this criterion, demonstrating that for a HIC score of 1000, there is a 16% probability of an AIS 4+ injury (**Figure 3**). A HIC score of 1500 corresponds to a 56% probability of an AIS 4+ head injury. Later analyses of these data resulted in the formulation of expanded risk curves that approximate the HIC distribution for each AIS injury severity level (21). Subsequent validation studies included reconstructions of real-world vehicle-to-pedestrian accidents, which have not only confirmed the validity of earlier cadaver work, but also demonstrated the reliability of using cadaveric specimens for head injury research (22). These experiments demonstrate an abrupt transition from moderate to severe head injury occurring over a HIC range of 1100 to 1400. The

Figure 3

Head injury risk curves based on HIC values.



data also show a 50% to 60% probability of an AIS 3+ head injury for HIC scores of 1000.

Head impact power. Although HIC is primarily used as a criterion for more severe head injury, various complimentary injury measures have been developed to assess less severe head injuries, such as mild traumatic brain injury (MTBI). MTBI, or concussion, is defined by the American Academy of Neurology as “a trauma-induced alteration in mental status that may or may not involve loss of consciousness” (23). The injury criteria used to assess MTBI range from simple single-axis translational and rotational criteria, such as the Generalized Model for Brain Injury Threshold (GAMBIT) (24, 25), to complex stress-strain dependent finite element (FE) models of the brain and its surrounding support structures, such as those proposed by Baumgartner et al. (26) and Miller et al. (27). Of the numerous MTBI injury metrics, the Head Impact Power (HIP) is appealing given its incorporation of full six-degree-of-freedom head kinematics, ease of use, and, most importantly, the extensive validation studies that have demonstrated good correlation with MTBI (28–30). The HIP is used to assess the change in translational as well as rotational kinetic energy of the head. In general form, this vector function can be expressed as

$$P = \sum m\dot{\mathbf{a}} \cdot \dot{\mathbf{v}} + \sum I\dot{\boldsymbol{\alpha}} \cdot \dot{\boldsymbol{\omega}} \text{ [kW]}, \quad (6)$$

where, with reference to the head, m is the mass, I is the rotational inertia, \mathbf{a} is the linear acceleration, \mathbf{v} is the linear velocity, $\boldsymbol{\alpha}$ is the angular acceleration, and $\boldsymbol{\omega}$ is the angular velocity. To determine HIP, this function is evaluated using the full six degrees of freedom (three translational and three rotational) for head motion. That is, the linear motion of the head along three axes as well as the rotational motion of the head around three axes are included in the calculation of the injury criterion. Expanding the formula, with the inertial coefficients assigned in accordance with appropriate

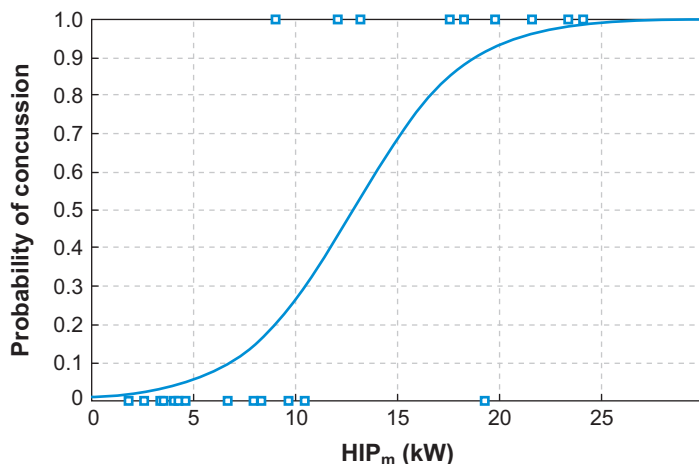


Figure 4
Probability of concussion based on HIP (29).

values for the human head, HIP can be expressed as

$$\begin{aligned} \text{HIP} = & 4.50a_x \int a_x dt + 4.50a_y \int a_y dt + 4.50a_z \int a_z dt \\ & + 0.016\alpha_x \int \alpha_x dt + 0.024\alpha_y \int \alpha_y dt + 0.022\alpha_z \int \alpha_z dt \text{ [kW]}. \quad (7) \end{aligned}$$

To validate the HIP injury criterion and determine the correlation with MTBI, researchers (14, 29) examined more than 100 helmet-to-helmet impacts occurring during North American professional football games in which at least one athlete sustained concussion symptoms. The games provided an excellent real-world laboratory for the study of brain injury, as the outcomes were diagnosed by medical staff and the impacts were captured on video film from multiple perspectives. Moreover, the research team had gathered preseason data using a variety of psychological and physiological questionnaires and measurements and could thus compare these data before and after MTBI. Of the 100 collisions studied, 12 impacts involving 24 players were reconstructed experimentally using instrumented anthropomorphic test devices. The impact orientations of each player, as well as the closing speed at impact, were determined from analysis of the game video footage. When a logistic risk curve was fit to the data, the 50% probability of concussion was identified at a HIP score of 12.8 kW (**Figure 4**). Close examination of the data points further demonstrates an extremely clean transition from no concussion to concussion occurring at approximately 10 kW.

Neck Injury Criteria

The neck injury criterion (termed N_{ij}) was proposed to the National Highway Traffic Safety Administration to assess neck injuries in frontal impacts and is currently the only neck injury criterion included in the federal motor vehicle safety standards. Current federal regulations do not specify a neck injury criterion for assessing the potential for injury from relatively minor rear-end and frontal collisions. However,

in forensic injury biomechanics, a second neck injury criterion (termed NIC) can be used to assess soft tissue neck injuries in such impacts.

Neck injury criteria. The N_{ij} included in the current FMVSS 208 frontal impact protection standard (19) accounts for the combination of axial loads and bending moments in the upper neck that is known to be associated with neck injury. Previous neck injury criteria included individual tolerance limits for axial loads and bending moments. The concept of an injury criterion utilizing a linear combination of axial load and bending moment was developed in the 1980's from experimental tests on pigs (31). For humans in a frontal collision, the primary neck loads occur in the sagittal plane. As a result, only the axial neck loads (compression and tension) and bending moments (flexion and extension) were considered significant, and this concept was later expanded to include the four major neck-loading modes: tension-extension, tension-flexion, compression-extension, and compression-flexion. The resulting criteria are referred to as N_{ij} , where ij represent indices for the four injury mechanisms. In developing the N_{ij} criteria, data produced in crash tests with instrumented human volunteers, cadavers, and dummies were used, in addition to a comparison of the results with real-world injury statistics. Forces and moments are normalized with respect to critical intercept values defined for tension, compression, extension, and flexion. The neck injury criterion is thus written as the sum of the normalized loads and moments,

$$N_{ij} = \frac{F_Z}{F_{INT}} + \frac{M_Y}{M_{INT}}, \quad (8)$$

where F_Z is the axial load, F_{INT} is the critical intercept value of load used for normalization, M_Y is the bending moment, and M_{INT} is the critical intercept value of moment used for normalization. The N_{ij} formula is the same regardless of dummy size because the critical values for normalization are scaled (**Table 2**).

The N_{ij} criterion was proposed to the National Highway Traffic Safety Administration (18, 32) to assess neck injuries in frontal impacts, and is currently the only neck injury criterion included in FMVSS 208. According to the FMVSS 208 frontal impact protection standard, N_{ij} must not exceed 1.0 at any point in time during a motor vehicle collision. Because the N_{ij} criterion is normalized, a value of 1.0 represents a 22% risk of an AIS 3 injury for all occupant sizes. Complete risk curves for AIS 2, 3, 4, and 5 neck injuries have been developed as a function of the calculated N_{ij} value (**Figure 5**).

Table 2 Critical intercept values for calculating N_{ij} (19)

Dummy	Tension	Compression	Flexion	Extension
50th percentile adult male	6806 N (1530 lb)	6160 N (1385 lb)	310 N-m (229 ft-lb)	135 N-m (100 ft-lb)
5th percentile adult female	4287 N (964 lb)	3880 N (872 lb)	155 N-m (114 ft-lb)	67 N-m (49 ft-lb)
6-year-old child	2800 N (629 lb)	2800 N (629 lb)	93 N-m (69 ft-lb)	37 N-m (27 ft-lb)
3-year-old child	2120 N (477 lb)	2120 N (477 lb)	68 N-m (50 ft-lb)	27 N-m (20 ft-lb)
12-month-old CRABI	1460 N (328 lb)	1460 N (328 lb)	43 N-m (32 ft-lb)	17 N-m (13 ft-lb)

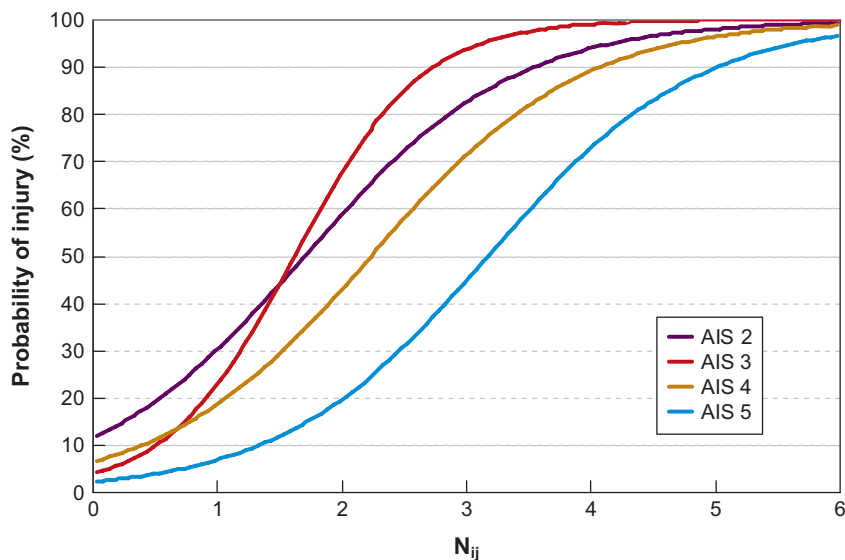


Figure 5
Neck injury risk curves based on N_{ij} values (33).

Neck injury criterion. Current federal regulations do not specify a neck injury criterion for assessing the potential for injury from relatively minor rear-end and frontal collisions. However, in forensic injury biomechanics, a neck injury criterion “NIC” can be used to assess soft tissue neck injuries in such impacts. NIC has recently been validated against real-world crash data for both rear (34) and frontal (35) collisions. NIC was first developed based on animal experiments, assuming that pressure changes inside the spinal canal were related to injury (36). These pressure changes were found to correlate with the rearward motion of the head, as the upper neck makes a quick transition from flexion to extension curvatures. The NIC, in its generic form, is defined as

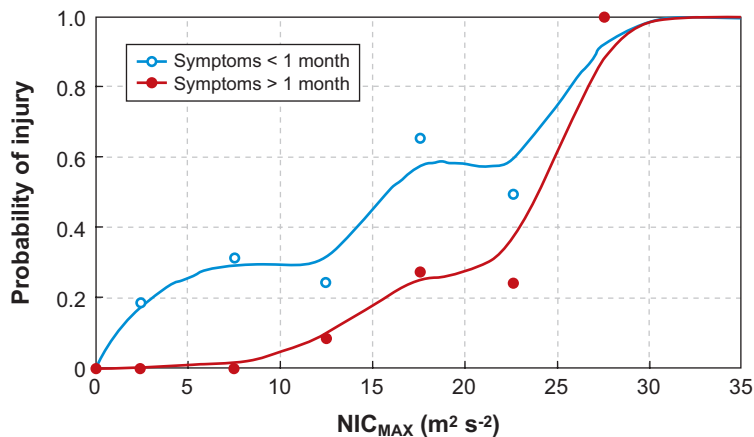
$$\text{NIC}_{\text{generic}}(t) = 0.2 \cdot a_{\text{rel}}(t) + v_{\text{rel}}(t) \cdot |v_{\text{rel}}(t)|, \quad (9)$$

where $a_{\text{rel}}(t)$ and $v_{\text{rel}}(t)$ represent the relative acceleration and velocity (as functions of time) between the head (measured at the top of the neck, C1) and torso (measured at the bottom of the neck, T1), respectively. The definition of NIC was then refined to account for rearward head motion prior to large head rotations, so that only the maximum value of NIC within the first 150 ms is used. Moreover, only the positive maximum value of NIC is considered because the negative values caused by contact with the head restraint do not produce injuries. The NIC_{max} was then defined as

$$\text{NIC}_{\text{max}} = \text{Maximum}_{\text{first 150 ms}} (0.2 \cdot a_{\text{rel}} + v_{\text{rel}}^2). \quad (10)$$

Based on validation studies involving reconstructions of real-world collisions, and both short- and long-term follow-up, NIC_{max} was found to correlate well with both short- and long-term AIS 1 neck injury symptoms (**Figure 6**). The threshold (i.e., greater than 50% probability) for short- and long-term symptoms corresponded to NIC values of 15 and 24 m^2/s^2 , respectively.

Figure 6
Neck injury risk versus NIC_{MAX} (34).



A modification of NIC, called $NIC_{protraction}$, has been used to evaluate AIS 1 neck injuries in frontal impacts (35, 37). The $NIC_{protraction}$ is defined as

$$NIC_{protraction} = |\text{Minimum } NIC_{generic}|. \quad (11)$$

Similar to NIC_{max} being validated for use in rear-end impacts, $NIC_{protraction}$ has been found to correlate well with AIS 1 neck injury symptoms in frontal impacts. The threshold for short- and long-term symptoms corresponded to $NIC_{protraction}$ values of 15 and 25 m^2/s^2 , respectively (37).

APPLICATIONS

Motor Vehicle Collisions

One of the most prevalent sources of traumatic injury for the general population is motor vehicle collisions. Although great advances have been made in the design of safe vehicles, roadway design, and operator education, thousands of Americans are injured or killed in motor vehicle collisions each year.

Three-step approach. To assess the biomechanics of injury in a motor vehicle collision, one must perform a three-step analysis. In the first step, the collision reconstruction, the type and severity of the collision must be determined. These parameters usually include the change in velocity of the vehicle (often referred to as delta-V) and associated acceleration time-history of the occupant compartment. Step two, the occupant dynamics analysis, consists of modeling the kinematics of the occupant along with the induced occupant loading when subjected to the acceleration environment determined in step one. This step is usually accomplished by implementing a three-dimensional, multi-link, dynamic simulation. Step three, the injury biomechanics analysis, consists of comparing the occupant loading states determined in step two with experimentally determined injury tolerance thresholds. Use of this three-step approach to injury assessment appears in governmental reports involving

accident investigation and in accident reconstruction and biomechanics literature (38–42).

Analysis tools/software. Analytical models and simulation tools are commercially available for the analysis of motor vehicle collisions (MVCs). One such set of models and tools is the Human Vehicle Environment (HVE) software suite distributed by Engineering Dynamics Corporation. The software includes various models that are used to analyze vehicle deformation, collision dynamics, rollover events, and occupant and pedestrian dynamics. Each model is based on automotive collision, safety, and component performance research. The models have been subjected to, in many cases, decades of peer-review and validation.

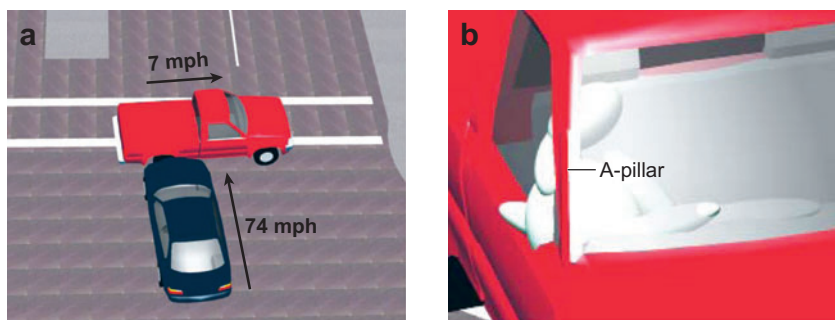
Of the vehicle collision models, the Engineering Dynamics Simulation Model of Automobile Collisions, version 4 (EDSMAC4) is widely used for collision reconstruction (43, 44). The model is appealing given its basis in fundamental physics and its extensive validation in peer-reviewed literature. Based on a program called Simulation Model of Automobile Collisions (SMAC) that was originally developed at Calspan for NHTSA, EDSMAC4 can be used to analyze single- or multiple-vehicle collisions. The simulation program uses a set of vehicle-specific parameters and preimpact initial conditions, including vehicle position, orientation, velocity, and heading. Output from the model includes postimpact vehicle trajectories, along with predicted damage profiles. Use of this simulation model is widely accepted in the collision reconstruction community and has been extensively validated for single-vehicle impacts with barriers and poles and rollover events, and for vehicle-vehicle interactions over a wide range of impact types and severity levels (45, 46). Error rates in the range of 2% to 7% are cited for these techniques.

The HVE suite also contains an occupant dynamics simulation model referred to as the Graphical Articulated Total Body (GATB). The GATB model is used to compute occupant kinematics (position, velocity, and acceleration versus time), joint angles and torques, and contact forces between the human occupant and contact panels placed in the interior of the vehicle. GATB is an extension of the ATB (Articulated Total Body) computer model, and is designed for use with the graphical user interface supported by HVE. Both the ATB and GATB occupant dynamics models, which share the same fundamental simulation coding, have been validated for modeling occupant dynamics for a wide range of complex events, including automobile rollovers and aircraft ejection (47–50). For ATB simulations of lower acceleration level rear-impact collisions, the model demonstrated occupant dynamics predictions with error rates between 2% and 17% (51). Our research group has also used the ATB model to study the biomechanics of hip fracture from falls (52).

High-speed T-bone collision. A 36-year-old male was the single occupant/operator of a Toyota pickup, executing a legal U-turn at an urban intersection. At the mid-point of the U-turn maneuver, the pickup was struck along the right side by an oncoming Mercedes sedan being operated at high speed by a drunk driver. The operator of the pickup was unrestrained at the time of impact. The collision dynamics resulted in the occupant's body translating laterally to the right and slightly forward,

Figure 7

Vehicle states (*a*) at initiation of collision simulation, and occupant dynamics simulation (*b*) depicting head impact with passenger side A-pillar roof support.



with respect to a vehicle-fixed reference frame. This resulted in the operator's head striking the passenger side A-pillar roof support column. Along with various extremity fractures, the operator sustained a severe, AIS 5, traumatic brain injury, ultimately resulting in death. At issue in this case was the type and severity of injuries that the operator would have sustained had he been using the available three-point seat belt restraint.

A conservation of momentum analysis of the vehicle and scene evidence indicated that at the time of impact, the Toyota pickup was traveling approximately 11 kph (7 mph), while the Mercedes sedan was traveling approximately 119 kph (74 mph). Using these impact speeds, vehicle inertial, stiffness, and geometric data, along with the known regions of vehicle interaction, the collision was simulated using commercially available, extensively validated, accident reconstruction analysis software. With the collision dynamics of the Toyota pickup determined, two separate occupant dynamic simulations were performed using GATB. For the unbelted simulation, the operator was positioned in the driver's seat, unrestrained, and subjected to the reconstructed collision pulse. As expected, upon exposure to the collision pulse, the operator translated laterally with respect to the vehicle, impacting the A-pillar (**Figure 7b**). The peak head acceleration was 357 g. The time history of head acceleration was retained for subsequent HIC analysis. For the belted case, the operator was again positioned in the driver's seat of the Toyota pickup and subjected to the previously defined collision pulse. However, for this simulation, a three-point seat belt restraint was simulated. Results demonstrated that the seat belt restraint retained the operator in the driver's seat and prevented head contact with any stiff structures of the vehicle. However, collision forces caused rapid and violent lateral bending and rotation along the operator's entire vertebral column. Simulation predictions indicated shearing forces in the lumbar spine in excess of 22.2 kN (5000 lbs) and tensile forces in excess of 57.8 kN (13000 lbs). With respect to the neck, flexion bending moments in excess of 813.5 N-m (600 ft-lbs) and tensile loading in excess of 2.2 kN (500 lbs) were also predicted.

Analysis of the head acceleration time history from the first, unrestrained, occupant dynamics simulation revealed a HIC score of more than 13000 (**Figure 8**). When compared with injury risk curves (**Figure 4**), this level of loading represents a greater than 99% probability of an AIS 5+ head injury. These results comported with the outcome of the actual collision and served as a validation of the analysis procedure.

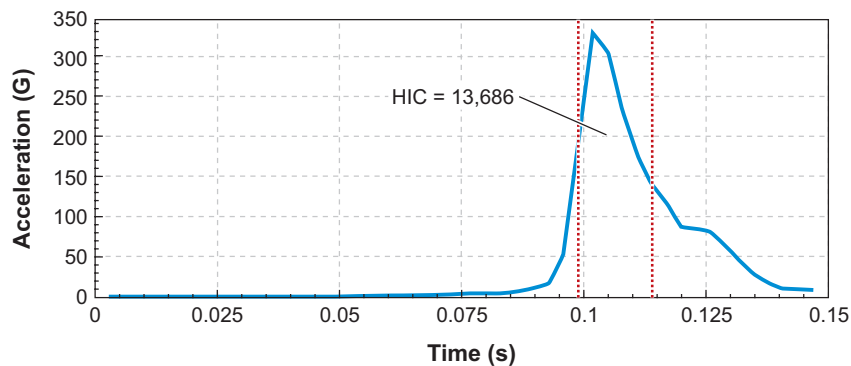


Figure 8
HIC analysis of A-pillar head strike.

Analysis of the neck loading predicted in the second, restrained, occupant dynamics simulation revealed an N_{ij} score of approximately 3.0. N_{ij} scores of this level represent a 53% probability of AIS 5+ neck injuries, which include complete cord syndrome with quadriplegia or paraplegia. With respect to lumbar loading, injury tolerance data for cord damage are scarce. However, the magnitude of the shear forces imposed on the lumbar spine, which are well in excess of applicable vertebral fracture tolerance data, is consistent with this type of injury. Our conclusion was that had the operator of the Toyota pickup been wearing a seat belt at the time of the collision, he would likely not have sustained a severe head injury, but would have sustained an AIS 5+ neck injury.

Head-on collision. A 49-year-old male was operating a Chevrolet sports car on a rural asphalt roadway. While executing a right-hand curve in the road, the sports car was met by an oncoming logging truck. The rear of the tractor-trailer was off-tracking into the lane occupied by the Chevrolet, resulting in a collision between the front left of the Chevrolet and the third axle of the tractor-trailer. Following the collision, the operator of the Chevrolet alleged that he sustained AIS 1 neck injuries. At issue was whether or not the AIS 1 neck injuries alleged by the operator of the Chevrolet sports car were consistent with the severity of the collision.

Vehicle crush damage, along with roadway evidence, was used to reconstruct the collision severity and corresponding vehicle dynamics. The speed of the tractor trailer was estimated to be between 24.1 kph (15.0 mph) and 29.0 kph (18.0 mph) at the time of impact. The Chevrolet had come to a complete stop prior to impact. The resultant change in velocity, referred to as delta-V, of the Chevrolet was 23.7 kph (14.7 mph), with a 17.2 kph (10.7 mph) rearward-directed longitudinal component. Using the vehicle collision dynamics determined from the collision reconstruction, a validated occupant dynamics model was used to predict the resulting occupant kinematics and kinetics. Simulation output demonstrated that the operator was forced forward and to the left with respect to the vehicle (**Supplemental Figure 2**). Chest and pelvis interaction with the seat belt, along with shoulder interaction with the interior surfaces of the driver's side door, restrained the occupant's torso movement. However, the relatively unrestrained head continued forward and to the left, inducing

combined forward and lateral bending on the driver's neck. The peak relative C1-T1 acceleration was approximately 13 g's, whereas the peak relative C1-T1 velocity was approximately 55 m/s (180 ft/s).

The NIC neck injury criterion was used to assess the correlation between the induced neck kinematics and the alleged injuries. The calculated NIC score for the collision event was 25 m²/s². Comparing this score with injury thresholds for long-term AIS 1 injury (25 m²/s²) and short-term AIS 1 injury (15 m²/s²) yielded factors of risk of 1.0 and 1.7, respectively. We concluded that the AIS 1 neck injuries alleged by the operator of the Chevrolet were consistent with occupant loading induced by the collision event.

Tractor-trailer collision. A 42-year-old male was the unrestrained operator of vehicle #1, a fully loaded tractor-trailer that was attempting to exit a business driveway. In the midst of pulling forward from the driveway, the front-left corner of vehicle #1 was struck by vehicle #2, a second tractor-trailer that was approaching from the right on the intersecting roadway. As a result of the collision, the operator of vehicle #1 sustained a minor nasal fracture, along with two 1-cm facial lacerations. Claims of blurred vision ultimately led to the diagnosis of a possible concussion. At issue in this case was whether the operator had sustained a MTBI with associated concussion. Also of interest was whether or not the nasal fracture would have occurred had the available lap and shoulder restraints been used.

The collision between the two tractor-trailers was reconstructed using a dynamic simulation (**Supplemental Figure 3**). Using the known vehicle parameters, along with postcollision scene evidence that identified the final rest positions and orientations of each articulated vehicle, the impact speeds and corresponding impact severity levels were established. The speed of vehicle #1 at impact was approximately 8 kph (5 mph), whereas the speed of vehicle #2 was between 19.3 kph (12.0 mph) and 23.0 kph (14.3 mph). The corresponding delta-V of vehicle #1 was between 8 kph (5 mph) and 11.3 kph (7 mph).

The occupant dynamics were analyzed for both the actual scenario in which the operator was unrestrained and the hypothetical scenario in which the operator was using the available three-point seat belt restraint. Simulation of the unrestrained scenario demonstrated that upon impact, the operator initially translated laterally to the left, with respect to the vehicle, striking the left side of his forehead on the driver's side door window. Parametric studies investigating varying degrees of preimpact leftward rotation of the operator's head revealed that contact between the operator's nose and the window was unlikely. Following this initial lateral motion, the operator was forced forward in response to the vehicle dynamics associated with the collision-induced motion of the tractor-trailer. The forward motion resulted in the occupant striking his face against the steering wheel and instrument panel (**Figure 9**).

The restrained scenario revealed that the operator's initial leftward motion and associated head contact with the driver's side window was essentially unchanged compared with the unrestrained scenario. This result comports with our understanding that a typical three-point seat belt would do little to prevent leftward motion of the head and its impact with the driver's window. However, three-point restraint use did

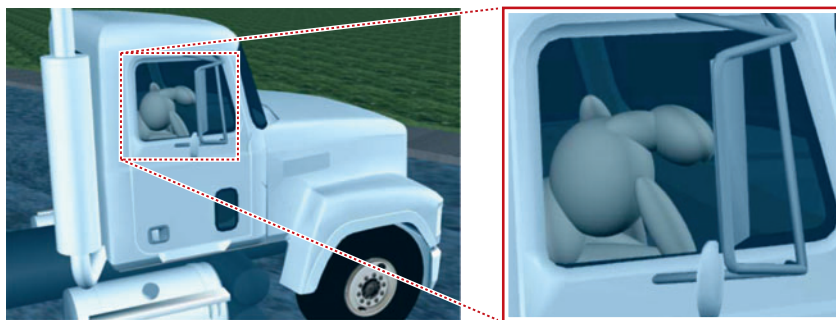


Figure 9
Occupant dynamics simulation depicting predicted instrument panel head strike.

prevent any significant forward movement of the operator during the latter phase of the event, completely eliminating the head contact with the steering wheel and instrument panel. The HIP injury criterion was also calculated to assess the likelihood of concussion occurring during the collision event. For the initial impact between the operator's head and the driver's side window, a HIP score of 3.2 kW was predicted. For the subsequent impact between the operator's head and the steering wheel/instrument panel, a HIP score of 5.9 kW was predicted. For each of these impacts, the probability of concussion was less than 10% (**Figure 10**). Given the low injury risk scores and the findings of Newman et al. (28) that not a single concussion was observed at HIP scores below 8 kW, we concluded that a concussion was not consistent with the collision event. Moreover, had the operator been wearing a seat belt restraint at the time of the collision, he would not have experienced that facial impact that caused the nasal fracture.

Slips, Trips, and Falls

The fundamental laws of physics are often used in forensic injury biomechanics to analyze the impact forces associated with falls. These laws include the conservation

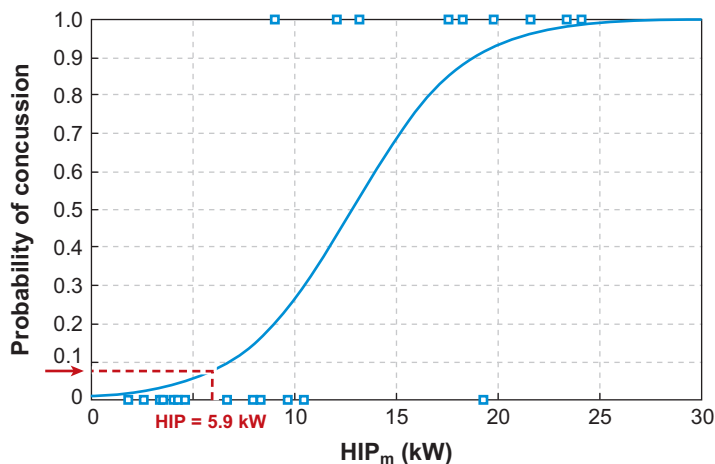


Figure 10
Probability of concussion.

of energy and impulse-momentum principles. If the descent height (h) of an object is known, its impact velocity (v) can be calculated according to

$$v = \sqrt{2gh}, \quad (14)$$

where g is the acceleration due to gravity. Similarly, if an object with a known height (h) is initially vertical and then rotates 90° (i.e., “topples” about its pivot point with the ground), the impact velocity experienced by the top of the object can be calculated according to

$$v = \sqrt{3gh}. \quad (15)$$

The impulse-momentum principle is often used to calculate impact forces. This is written as

$$F\Delta t = (q)m\Delta v. \quad (16)$$

This principle states that, if a force (F) is applied to a mass (m) for a given duration (Δt), the product of this force and its duration of application (i.e., the impulse) is equal to the product of the mass and the change in velocity (Δv) experienced by the object (i.e., the momentum). The factor (q) is multiplied by the momentum ($m\Delta v$) to account for any rebound effects at impact, and is a value between one and two. The impact duration is a function of stiffness of the impacting objects. For example, impacts to the adult human skull have a shorter duration than those to the soft tissues surrounding the buttocks. Impact, or contact durations, for various anatomic regions is often obtained from published experimental test data involving cadavers. Therefore, if an object is brought to rest upon impact, and its effective mass (defined as that fraction of the total body mass that actually participates in the impact) and the impact duration and velocity are known, then the impulse-momentum principle can be used to calculate the impact force.

In addition to motor vehicle collisions, multilink biodynamic models are also used to simulate slips, trips, and falls. A more complete review of these mathematical models has been published by Prasad & Chou (53). One example is the physics-based program called Working Model, which has been used to analyze both mechanical and biomechanical systems (54–59). The program provides an organized approach to writing the equations of motion for multicomponent, dynamic systems, and is therefore based on the extensively validated physical laws of engineering dynamics. Another widely used model is the ATB program, which is also described in the previous section on motor vehicle collisions. The ATB model has been used to study human falls (52, 60), and its predictions have been validated against experimental results for actual falls in volunteers (61, 62). These studies demonstrated that the predictions made by the ATB model were within roughly 20% of actual measurements from falls experienced by human volunteers. This research with human volunteers (61) also examined fall direction (forward, sideways, backward) as a function of the disturbance type (faint, slip, step down, trip) and gait speed (fast, normal, slow). It was demonstrated that trips predominantly produce forward falls (93%–100%), whereas slips produce sideways or backward falls (72%–79%).

Fall from standing height. A 61-year-old female was walking down the left side of a ramp at her place of employment. She was wearing low-heeled shoes. There was no water or foreign substance present on the ramp. Halfway down the ramp, she allegedly slipped and fell forward onto her right knee, fracturing her right patella. In addition to the biomechanics of her knee injury, at issue was whether she slipped or if she instead tripped and fell forward. The knee impact velocity was calculated using conservation of energy principles ($v = \sqrt{2gh}$). The force imposed on the woman's right knee as a result of the impact was determined using the impulse-momentum principle [$F\Delta t = (q)m\Delta v$], with the impact velocity, her effective body mass, and contact duration for patellar impacts as input parameters.

Based on the length of her lower leg, her right patella would have impacted the floor with a velocity of approximately 3 m/s (10 ft/s). Given her effective body mass of 50 kg (110 lbs) (total body weight – right lower leg), and a patellar contact time of 0.01 s (63), her right patella was subjected to an impact force of 15 kN (3400 lbs). Patellar fractures have been experimentally produced (64) for impact forces between 5.3 kN (1200 lbs) and 9.3 kN (2100 lbs). Therefore, regarding her knee injury, the factor of risk was between 1.6 and 2.8.

The woman's medical records contained conflicting descriptions of the event. She described herself as tripping on a heel, in addition to slipping and landing on her right knee. Upon further review of her medical records, several risk factors for falling were also identified, including a fractured left first toe that was diagnosed just weeks before the incident occurred (65), her use of antidepressant drugs (66), and the geometry of her shoe heels (67). The coefficient of friction between her shoes and the ramp was also determined to be greater than that necessary while walking down the 5° ramp (68). Based on all of these factors, and the previous research (61) demonstrating that trips predominantly produce forward falls (93%–100%), whereas slips produce sideways or backwards falls (72%–79%), we concluded that the woman fractured her patella as a result of tripping rather than slipping, causing her to fall forward and land on her right knee.

Fall off an exercise bicycle. A 59-year-old male was using a stationary exercise bicycle when he began having an episode of ventricular tachycardia, which caused his internal cardioverter defibrillator to deliver a high-energy shock directly to his heart. He was knocked off the bicycle, causing him to strike his head on the vinyl composite tiled floor. A witness saw the man fall head-first off the bicycle. He sustained a laceration on his left forehead, but no skull fractures. The man was also taking Coumadin medication, and eventually died from an expanding subdural hematoma. To determine the impact force between the man's head and the floor, injury risk curves as a function of HIC, skull fracture tolerance limits, and the AIS scale were used. The POD was calculated by assigning AIS scores to each of his injuries. Various protective measures were also evaluated to determine whether or not the man's death would have been prevented had such measures been in place.

According to the AIS (8), the initiation of a subdural hematoma is assigned an AIS score of 3. Previous cadaver experiments have determined a fracture tolerance of 6400 N (1440 lbs) for the frontal bone, when allowed to fall and impact a flat, rigid

surface (69). In these experiments, HIC was calculated to be approximately 1000. As described above in the head injury criterion section, injury risk curves yield a 50% to 60% probability of an AIS 3+ head injury for a HIC score of 1000 (21, 22). Therefore, we concluded that the decedent's head experienced an impact force of approximately 6200 N (1400 lbs), which initiated his subdural hematoma without producing a skull fracture.

In addition to the injuries already mentioned, the decedent also sustained bruises and an abrasion to his chest. These relatively minor injuries were assigned an AIS score of 1. His expanding subdural hematoma would be coded as either a 4 or 5, depending on its volume. Based on these AIS scores to the man's head and chest, and his age of 59 years, he had a 49% to 93% probability of death (70) as a result of his injuries. We therefore concluded that the man's death was consistent with an expanding subdural hematoma. Various protective measures were also available, including floor padding, a bicycle helmet, and a recumbent cycle. The floor padding would have increased the contact duration, thus dramatically reducing the head impact force experienced by the decedent. Bicycle helmets are effective at preventing serious head injuries by attenuating the impact force. A recumbent cycle seats the user much closer to the ground, which would have reduced the descent height, and thus the head impact velocity and force. We concluded that, had any of these protective measures been used, the initiation of the decedent's subdural hematoma, which ultimately led to his death, would have been prevented.

Fall from a balcony. A 57-year-old male was found dead on the ground below a balcony [height = 8.92 m (29.25 ft)]. He sustained compound fractures near both knees, a severe laceration to his forehead, a fractured nasal bone, and subdural hemorrhaging. The cause of death was determined to be multiple traumatic injuries. The decedent had a history of seizures, including episodes of suddenly staggering forward and falling to the floor. The case question was whether or not the man could have fallen from the balcony as a result of a seizure. The physics-based simulation program, Working Model 2D v4.0.1, was used to reconstruct the kinematics of the fall (**Figure 11**). A mathematical surrogate representing the man's height and weight was included in the model, as well as the balcony dimensions and slope of the landing. The surrogate was assigned an initial forward velocity of approximately 2 m/s (6.6 ft/s) to simulate a seizure as he approached the balcony railing.

The simulation indicated that initial contact occurred between the top balcony edge and the subject's legs, just above the knees, which was consistent with a horizontal, linear contusion found at that location. The simulation then predicted the following impacts with the ground, in sequential order: toes, knees, and then face. Each of these impacts was consistent with his actual injuries, including the contusions to his toes, bilateral femur fractures, and a fractured nasal bone. The forces associated with the knee and facial impacts were calculated using the impulse-momentum principle [$F\Delta t = (q)m\Delta v$] and found to be above the respective fracture tolerance levels, further validating the analyses. Finally, he had a 86% POD (70) as a result of his age (57 years old) and the severity of his multiple injuries (bilateral lung contusions = AIS 4,

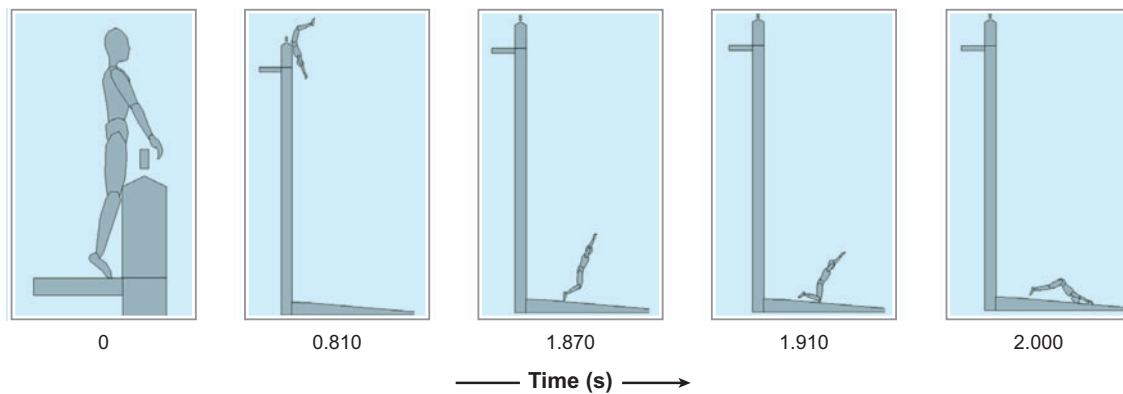


Figure 11

Simulation of the fall from a balcony kinematics.

femoral fractures = AIS 3). Our conclusion was that the man fell from the balcony as a result of a seizure.

Catastrophic neck injury from low-height trampoline jumps. A 40-year-old male reported to emergency personnel at the scene that he had been bouncing



Figure 12

C4/5 fracture subluxation of the cervical spine.

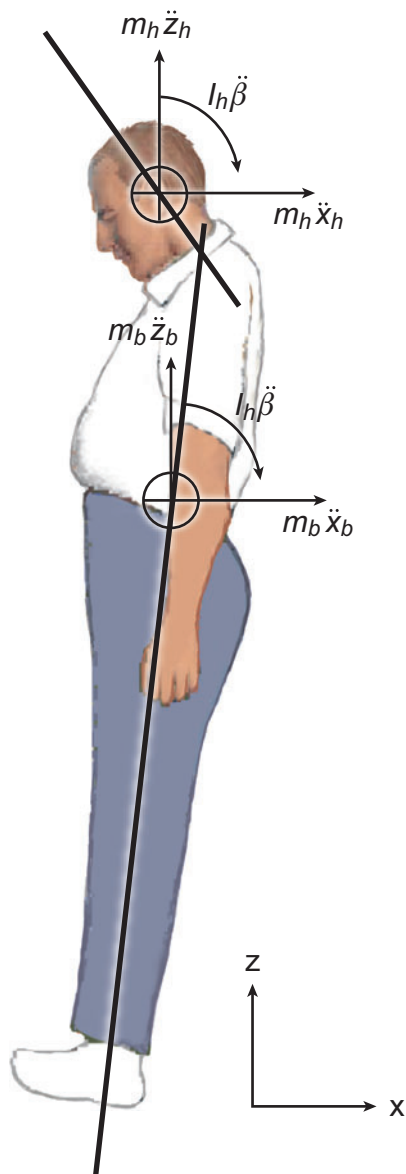


Figure 13

Two-link biomechanical model.

vertically, somewhat stiff-legged, a few inches off a backyard trampoline, when his feet slipped rapidly out from under him, causing him to rotate backward and strike the back of his head on the trampoline mat. He further indicated that it was the first time he had been on a trampoline. He was subsequently found to have sustained a C4/5 fracture subluxation (**Figure 12**) accompanied by a spinal cord injury that

resulted in quadriplegia and permanent neurologic deficit. Based on his history, our goal was to determine whether a slip and backward fall, even when bouncing gently on a trampoline, was a plausible mechanism for this injury.

The subject was modeled as two rigid bodies connected with a planar pin joint at the neck (**Figure 13**). The neck joint in turn was modeled using a torsional spring and damper with properties chosen based on literature values. The AIS was used to describe the severity of the neck injury as an AIS 3. The predicted neck forces from the mathematical model were compared against the tolerance limits for the human cervical spine, using N_{ij} , where ij represents indices for compression and flexion. We also conducted validation experiments using a Hybrid III crash dummy, representing a fifth percentile female (**Figure 14**). Dummy kinematics from drop experiments onto an exemplar trampoline were digitized from high-speed video. Trampoline stiffness and damping were determined by dropping a bowling ball from various heights.

There was excellent agreement (within a few percent) between the angular orientation measured during experiments with the Hybrid III dummy and the angular orientation from the simulation (**Figure 14**). The dummy was nearly vertical initially and then rotated backward rapidly after initial impact of the feet on the trampoline mat. This resulted in impact to the back of the head. For the 95th percentile male involved in the incident under litigation, the predicted kinematics were similar, with a rapid backward rotation as the slipping feet were accelerated vertically by the rebounding mat. As the back of the head contacted the mat, vertical forces resulted in flexion moments on the cervical spine sufficient to exceed neck injury

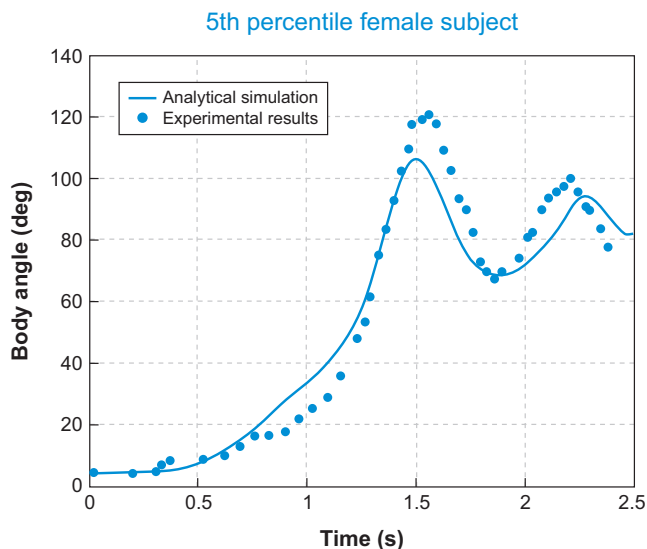
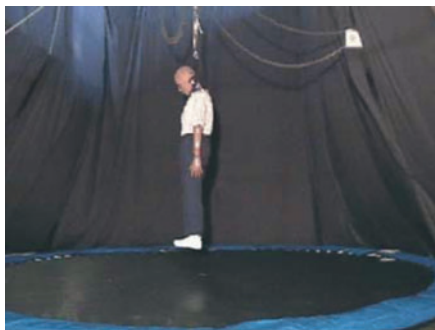
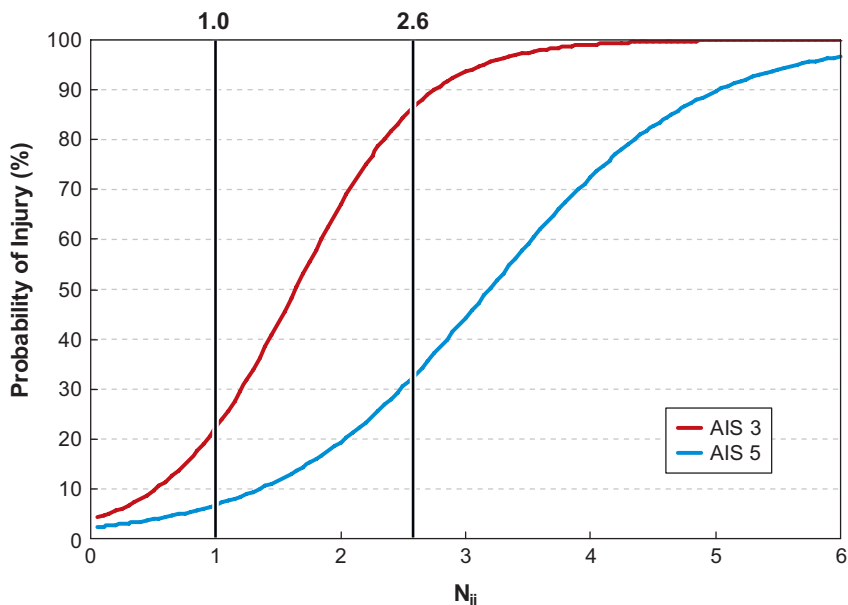


Figure 14

Validation experiment for biomechanical model showing 5th percentile female ATD. Agreement arises between experimental results and the analytical model. Based on this agreement, the model was used to extend the results to a 95th percentile male.

Figure 15

Probabilities of AIS 3 and 5 cervical spine injuries for the 95th percentile male involved in the trampoline accident.



criteria (**Figure 15**). With $N_{ij} = 1.0$ (i.e., at the injury threshold), the probabilities of AIS 3 and 5 injuries are only approximately 22% and 7%, respectively. However, at $N_{ij} = 2.6$ for the 95th percentile male, the probabilities for AIS 3 and 5 injuries are approximately 87% and 33%, respectively, thereby comporting with the injuries he actually sustained. These results demonstrate a serious injury mechanism peculiar to trampolines. When slipping and falling backward while bouncing, even gently, on a trampoline, the subject can be flipped backward by a strong upward force exerted by the trampoline mat on the slipping feet. This causes the body to rotate through a large angle so that the head directly impacts the trampoline surface, producing loads on the head sufficient to result in catastrophic injury to the cervical spine. We therefore concluded that the incident description provided by the subject was the likely mechanism for his injury and that he had not, as had been alleged, been attempting a back flip the first time he had set foot on a trampoline.

SUMMARY

Forensic injury biomechanics is the application to litigation of the science that relates mechanical forces to disruption of anatomical regions of the human body. An expert, if qualified by "... knowledge, skill, experience, training or education ..." may testify at trial in the form of an opinion if "... scientific, technical or other specialized knowledge ..." will assist the jury in understanding the evidence or determining a fact at issue. Such opinions must be stated in a manner appropriate for litigation, which, in civil trials, is a "more likely than not," or "at least 51% likely" basis. The scientific principles and methods relied upon by such experts must result in valid

and appropriately accurate conclusions, a requirement that is addressed by a series of legal decisions known as *Daubert* and their progeny. The *Daubert* criteria include (a) whether the methodology used by the expert can be, and has been, tested; (b) whether the theory or methodology has been subjected to peer-review and publication; (c) whether there is a known (and appropriate) rate of error for the method; and (d) whether the methodology is accepted within a relevant scientific community.

An opinion as to whether an event causes one or more injuries is grounded first in what is meant by causation; second, in how injuries can be characterized; and third, in how quantitative injury assessments can be related to mechanical forces. The criteria necessary to support an opinion on injury causation in an individual include (a) that the injury follow the event in an appropriate temporal sequence, (b) that there is direct, objective evidence of both exposure and injury, and (c) that the forces imposed on the anatomic structure at issue be sufficiently high to exceed the strength or tolerance limits of the region. The AIS was originally developed in the mid-1960s as a system to describe the severity of injuries throughout the body. The AIS is an ordinal scale ranging from 1 (minor) to 6 (maximum—currently untreatable). The AIS is a threat to life ranking, with higher AIS levels indicating an increased threat to life. Data demonstrate that there is a strong, nonlinear correlation between AIS severity and survival (as well as mortality). Because the AIS is not designed to assess the combined effects of multiple injuries, the ISS has been developed to do so. The ISS scale is the sum of the squares of the highest AIS scores in three different body regions. Similarly, the POD makes use of AIS scaling with several modifications. The POD is calculated based on the two highest AIS values rather than three, AIS values are assigned for soft tissue and bony injuries, and the subject's age is taken into account.

The simplest, and most intuitively obvious, approach to predicting injury risk makes use of the ratio between the loads imposed on an anatomic structure and the ultimate load-carrying capacity of that structure. This approach can be formalized by defining a factor of risk, Φ , as the ratio of the applied loads divided by the loads necessary to cause injury. For a factor of risk well under one, injury is considered unlikely. For a factor of risk well in excess of one, injury is considered likely. This approach to injury risk prediction is also useful because it allows isolation of those factors that influence the numerator of the factor of risk (the loading factors) from those that influence the denominator (the factors that influence the vulnerability of the anatomic region to injury). To incorporate the variability inherent in both loading and tolerance data, injury risk functions are used. These probability functions can be used to express that level of the injury criterion for which injury is more likely than not (i.e., at least 51% probable).

Validated, widely accepted injury criteria are available for those anatomic regions (such as the head and neck) that are often injured and therefore are often involved in litigation. The HIC is based on a long history of research (involving experimental animals, human volunteers, and human cadavers) into those factors that cause serious injuries to the skull and brain. The current criterion that is incorporated into the FMVSS 208 reflects the combined effects of the magnitude of acceleration and the time over which the acceleration acts. The current criterion incorporated into the standard is that a 50th percentile male ATD is exposed to HIC scores of less than

700 and 1000, evaluated over maximum time intervals of 15 ms and 36 ms, respectively. Based on extensive validation experiments, a HIC score of 1000 results in a 16% probability of an AIS 4+ injury. A HIC score of 1500 corresponds to a 56% probability of an AIS 4+ head injury. Because HIC is primarily used as a criterion for severe head injuries, various complementary injury measures have been developed to assess the probability of concussion and MTBI. Of the numerous MTBI injury measures, the HIP is appealing because it incorporates the full motion of the head and has been demonstrated in experimental studies to correlate well with MTBI. Based on extensive studies of National Football League players, 50% probability of concussion occurred at a HIP score of 12.8 kW. Moreover, there was an extremely clean transition from no concussion to concussion that occurred at approximately 10 kW.

The neck injury criterion (N_{ij}) included in the current FMVSS 208 Frontal Impact Protection Standard accounts for the combination of axial loads and bending moments in the upper neck that has been proven in validation studies to be associated with neck injury. For humans in a frontal collision, the primary neck loads occur in the sagittal plane, resulting in combinations of axial neck loads (compression and tension) and bending moments (flexion and extension). Injuries thus occur in the neck under the loading combinations of tension-extension, tension-flexion, compression-extension, and compression-flexion. The resulting criteria are referred to as N_{ij} , where the ij represent indices for the four injury mechanisms. N_{ij} is written as the sum of normalized loads and moments. According to FMVSS 208, N_{ij} must not exceed 1.0 at any point in time during a motor vehicle collision. Because the N_{ij} criterion is normalized, a value of 1.0 represents a 22% risk of an AIS 3 injury for all occupant sizes. The value of N_{ij} for a 50% probability for an AIS 4 neck injury is 2.25.

Current federal regulations do not specify neck injury criterion for assessing injury potential for relatively minor rear and frontal collisions. However, because the causation of such injuries is often at question in litigation, considerable attention has been paid to risk factors for soft tissue injuries of the neck. NIC is widely used for this purpose. NIC has recently been validated against real-world crash data for both rear and frontal collision. NIC was first developed based on animal experiments that demonstrated pressure changes inside the spinal canal that were found to correlate with the rearward motion of the head as the upper neck makes the quick transition from flexion to extension curvatures. The NIC criterion represents the relative acceleration and velocity (as functions of time) between the head (measured at the top of the neck) and torso (measured at the bottom of the neck). Based on validation studies involving reconstructions of real-world collisions and short- and long-term clinical follow-up, NIC was found to correlate well with both short- and long-term AIS 1 neck injury symptoms. The threshold (i.e., at least 51% probability) for short- and long-term symptoms (with short-term being defined as less than one month) corresponded to NIC values of 15 and 24 m^2/s^2 , respectively.

DISCLOSURE STATEMENT

The authors are not aware of any biases that might be perceived as affecting the objectivity of this review.

LITERATURE CITED

1. Babitsky S, Mangraviti JJ, Todd CJ. 2002. *The Comprehensive Forensic Services Manual*. Falmouth, MA: SEAK, Inc.
2. Brautbar N. 1999. Science and the law: scientific evidence, causation, admissibility, reliability. "Daubert" decision revisited. *Toxicol. Ind. Health* 15:532-51
3. Hill AB. 1965. The environment and disease: association or causation? *Proc. R. Soc. Med.* 58:295-300
4. Bombardier C, Kerr MS, Shannon HS, Frank JW. 1994. A guide to interpreting epidemiologic studies on the etiology of back pain. *Spine* 19:S2047-56
5. Civil ID, Schwab CW. 1988. The Abbreviated Injury Scale, 1985 revision: a condensed chart for clinical use. *J. Trauma* 28:87-90
6. Wismans JSHM, Janssen EG, Beusenberg M, Koppens WP, Happee R, Bovendeerd PHM. 2000. *Injury biomechanics, Lect. notes college 47610*. Eindhoven, Netherlands: Eindhoven Univ. Tech.
7. Pike JA. 1990. *Automotive Safety: Anatomy, Injury, Testing and Regulation*. Warrendale, PA: SAE
8. Gennarelli TA, Wodzin E. 2005. *Abbreviated Injury Scale (AIS) 2005*. Barrington, IL: Assoc. Adv. Automot. Med. (AAAM)
9. Somers RL. 1983. The probability of death score: an improvement of the injury severity score. *Accid. Anal. Prev.* 15:247-57
10. Hayes WC, Myers ER, Robinovitch SN, van den Kroonenberg A, Courtney AC, McMahon TA. 1996. Etiology and prevention of age-related hip fractures. *Bone* 18:S77-86
11. Kent RW, Funk JR. 2004. Data censoring and parametric distribution assignment in the development of injury risk function from biomechanical data. *SAE 2004-01-0317*, pp. 1-11
12. Di Domenico L, Nusholtz G. 2005. Risk curve boundaries. *Traffic Inj. Prev.* 6:86-94
13. Gurdjian E, Webster J, Lissner H. 1949. Studies on skull fracture with particular reference to engineering factors. *Am. J. Surg.* 78(5):736-42
14. King AI. 2000. Fundamentals of impact biomechanics—Part 1: Biomechanics of the head, neck, and thorax. *Annu. Rev. Biomed. Eng.* 2:55-81
15. Fan WRS. 1971. Internal head injury assessment. *Proc. 15th Stapp Car Crash Conf.*, pp. 645-65
16. Gadd CW. 1966. Use of a weighted-impulse criterion for establishing injury hazard. *Proc. 10th Stapp Car Crash Conf., SAE Pap. 660793*, pp. 164-74
17. Versace J. 1993. A review of the severity index (710881). In *Biomechanics of Impact Injury and Injury Tolerances of the Head-Neck Complex (SAE PT-43)*, ed. SH Backaitis, pp. 309-34. Warrendale, PA: SAE
18. Kleinberger M, Sun E, Eppinger R, Kuppa S, Saul R. 1998. Development of improved injury criteria for the assessment of advanced automotive restraint systems. *NHTSA Doc. 98-4405-9*
19. Natl. Highw. Traffic Saf. Adm. (NHTSA). 2005. *Federal Motor Vehicle Safety Standards: Occupant crash protection, FMVSS 571.208, Stand. No. 208*, pp. 567-653

20. Prasad P, Mertz H. 1985. The position of the United States delegation to the ISO working group 6 on the use of HIC in the automotive environment. *SAE Pap.* 851246
21. Natl. Highw. Traffic Saf. Adm. (NHTSA). 1995. *Final economic assessment, upper interior head protection*. FMVSS No. 201
22. MacLaughlin TF, Wiechel JF. 1993. Head impact reconstruction—HIC validation and pedestrian injury risk. *SAE Pap.* 930895, pp. 175–82
23. Quality Stand. Subcomm. 1997. Practice parameter: the management of concussion in sports (summary statement). *Neurology* 48:581–85
24. Newman JA. 1986. A generalized acceleration model for brain injury threshold (GAMBIT). *SAE 1986-13-0008*, pp. 121–31
25. Newman JA. 1998. Kinematics of head injury. In *Frontiers in Head and Neck Trauma*, ed. N Yoganandan, FA Pintar, SJ Larson, A Sances Jr, pp. 200–14. Amsterdam, Netherlands: IOS Press
26. Baumgartner D, Willinger R, Shewchenko N, Beusenberg M. *Tolerance limits for mild traumatic brain injury derived from numerical head impact replication*. ULP-CNRS 7507, France: Strasbourg Univ.; Ottawa, Ontario, Can.: Biokinetics & Associates, Ltd.
27. Miller RT, Margulies SS, Leoni M, Nonaka M, Chen X, et al. 1998. Finite element modeling approaches for predicting injury in an experimental model of severe diffuse axonal injury. *SAE Pap.* 983154, pp. 1–13
28. Newman JA, Shewchenko N, Welbourne E. 2000. A proposed new biomechanical head injury assessment function—the maximum power index. *SAE Pap.* 2000-01-SC16, pp. 1–34
29. Newman JA, Barr C, Beusenberg M, Fournier E, Shewchenko N, et al. 2000. A new biomechanical assessment of mild traumatic brain injury. Part 2—results and conclusions. *SAE Pap.* 2000-13-0017, pp. 2–12
30. Newman JA, Beusenberg M, Fournier E, Shewchenko N, King A, et al. 1999. A new biomechanical assessment of mild traumatic brain injury. Part I—methodology. *SAE 1999-13-0001*, pp. 17–36
31. Prasad P, Daniel RP. 1984. A biomechanical analysis of head, neck, and torso injuries to child surrogates due to sudden torso acceleration. *SAE 841656*, pp. 25–40
32. Klinich KD, Saul RA, Auguste G, Backaitis S, Kleinberger M. 1996. Techniques for developing child dummy protection reference values. *NHTSA Doc.* 74-14, Notice 97, Item 069 1-7-5
33. Eppinger R, Sun E, Bandak F, Haffner M, Khaewpong N, et al. 1999. Neck injury criteria. In *Development of Improved Injury Criteria for the Assessment of Advanced Automotive Restraint Systems - II*, ed. R Eppinger, E Sun, F Bandak, M Haffner, N Khaewpong, et al., pp. 3-1–23. Washington, DC: NHTSA
34. Kullgren A, Eriksson L, Boström O, Krafft M. 2003. Validation of neck injury criteria using reconstructed real-life rear-end crashes with recorded crash pulses. Proc. 18th Int. Tech. Conf. Enhanced Safety Veh. (ESV), Nagoya, Jpn.
35. Boström O, Bohman K, Haland Y, Kullgren A, Krafft M. 2000. New AIS1 long-term neck injury criteria candidates based on real frontal crash analysis. *Int. Res. Counc. Biomechan. Impact., Montpellier, Fr.*

36. Boström O, Svensson MY, Aldman B, Hansson HA, Haland Y, et al. 1996. A new neck injury criterion candidate—based on injury findings in the cervical spinal ganglia after experimental neck extension trauma. *SAE 1996-13-0009*, pp. 123–26
37. Bohman K, Boström O, Haland Y, Kullgren A. 2000. A study of AIS1 neck injury parameters in 168 frontal collisions using a restrained hybrid III dummy. *SAE 2000-01-SC08*, pp. 1–14
38. Obergefell LA. 1995. Computer simulation of human body dynamics. *J. Gravit. Phys.* 2:92–95
39. Digges KH. 1984. Reconstruction of frontal accidents using the CVS-3D model. *SAE 840869*, pp. 151–64
40. Clark CC, Jettner E, Digges K, Morris J, Cohen D, Griffith D. 1987. Simulation of road crash facial lacerations by broken windshields. *SAE 870320*, pp. 175–97
41. Natl. Transp. Saf. Board. 2004. *Highway Accident Report: 15-Passenger Child Care Van Run-Off-Road Accident, Memphis, Tenn., April 4, 2002*. PB2004-916202, pp. 1–56
42. Natl. Transp. Saf. Board. 1999. *Highway Special Investigation Report: Bus crashworthiness*. NTSB/SIR-99/04, PB98-917006, pp. 1–152
43. Day TD, Hargens RL. 1988. An overview of the way EDSMAC computer delta-V. *SAE Pap.* 88-0069
44. Day TD, Siddall DE. 1996. Three-dimensional reconstruction and simulation of motor vehicle accidents. *SAE 960890*, pp. 211–19
45. Day TD, Hargens RL. 1990. Further validation of EDSMAC using the RICSAC staged collisions. *SAE 900102*, pp. 39–55
46. Day TD, Siddall DE. 1996. Validation of several reconstruction and simulation models in the HVE scientific visualization environment. *SAE 960891*, pp. 221–30
47. Prasad P, Chou CC. 1993. A review of mathematical occupant simulation models. In *Accidental Injury: Biomechanics and Prevention*, ed. AM Nahum, JW Melvin, Chapter 6, pp. 102–50. New York: Springer-Verlag
48. Grimes WD. 1995. Using ATB in collision reconstruction. *SAE 950131*, pp. 1–9
49. Cheng H, Rizer AL, Obergefell LA. 1995. ATB model simulation of a rollover accident with occupant ejection. *SAE 950134*, pp. 21–31
50. Grimes WD. 1997. Using ATB under the HVE environment. *SAE 970967*, pp. 395–403
51. Ojalvo IU, Yanowitz H. 1998. Vehicle and occupant response to low speed impact: comparison of analysis with test and parametric study. *SAE Pap.* 980300, pp. 1–12
52. Smeesters C, Hayes WC, McMahon TA. 2006. Determining the threshold trip duration using the articulated total body model. *J. Biomech. Eng.* In press
53. Prasad P, Chou CC. 2000. A review of mathematical occupant simulation models. In *Accidental Injury: Biomechanics and Prevention*, ed. AM Nahum, JW Melvin, Chapter 7, pp. 121–86. New York: Springer-Verlag
54. DiAngelo DJ, Evans CE. 1999. Design of a sports knee prosthesis. *ASME Bioeng. Div. BED* 43:295–96

55. Kamper D, Barin K, Parnianpour M, Hemami H, Weed H. 2000. Simulation of the seated postural stability of healthy and spinal cord-injured subjects using optimal feedback control methods. *Comput. Methods Biomech. Biomed. Eng.* 3:79–93
56. Kovler M, Lundon K, McKee N. 2004. The human first carpometacarpal joint: osteoarthritic degeneration and 3-dimensional modeling. *J. Hand Ther.* 17:393–400
57. Leardini A, Moschella D. 2002. Dynamic simulation of the natural and replaced human ankle joint. *Med. Biol. Eng. Comput.* 40:193–99
58. Pinkney S, Fernie G. 2001. Product development: using a 3D computer model to optimize the stability of the rocket powered wheelchair. *Assist. Technol.* 13:46–58
59. To CS, Kirsch RF, Kobetic R, Triolo RJ. 2004. The feasibility of a functional neuromuscular stimulation powered mechanical gait orthosis with coordinated joint locking. *Proc. Annu. Int. Conf. IEEE EMBS* 26(VI):4041–44
60. Smeesters C, Hayes WC, McMahon T. 2006. Determining fall direction and impact location for various disturbances and gait speeds using the articulated total body model. *J. Biomech. Eng.* In revision
61. Smeesters C, Hayes W, McMahon T. 2001. Disturbance type and gait speed affect fall direction and impact location. *J. Biomech.* 34:309–17
62. Smeesters C, Hayes WC, McMahon TA. 2001. The threshold trip duration for which recovery is no longer possible is associated with strength and reaction time. *J. Biomech.* 34:589–95
63. Powell W, Ojala S, Advani S, Martin R. 1975. Cadaver femur responses to longitudinal impacts. *SAE Pap. 751160*, pp. 561–79
64. Nyquist GW. 1986. Injury tolerance characteristics of the adult human lower extremities under static and dynamic loading. *SAE 861925*, pp. 79–90
65. Chen HC, Ashton-Miller JA, Alexander NB, Schultz AB. 1991. Stepping over obstacles: gait patterns of healthy young and old adults. *J. Gerontol.* 46:M196–203
66. Nevitt MC. 1997. Falls in the elderly: risk factors and prevention. In *Gait Disorders of Aging: Falls and Therapeutic Strategies*, ed. JC Masdeu, L Sudarsky, L Wolfson, Chapter 2, pp. 13–36. Philadelphia, PA: Lippincott-Raven
67. Tencer AF, Koepsell TD, Wolf ME, Frankenfeld CL, Buchner DM, et al. 2004. Biomechanical properties of shoes and risk of falls in older adults. *J. Am. Geriatr. Soc.* 52:1840–46
68. Redfern MS, Cham R, Gielo-Perczak K, Gronqvist R, Hirvonen M, et al. 2001. Biomechanics of slips. *Ergonomics* 44:1138–66
69. Hodgson VR, Thomas LM. 1973. Breaking strength of the human skull vs impact surface curvature. *NHTSA Rep. DOT/HS-801 002*, pp. 1–185
70. Pike JA. 1990. Injury scaling. See Ref. 7, pp. 47–60



Contents

Cell Mechanics: Integrating Cell Responses to Mechanical Stimuli <i>Paul A. Janmey and Christopher A. McCulloch</i>	1
Engineering Approaches to Biomaniplulation <i>Jaydev P. Desai, Anand Pillarisetti, and Ari D. Brooks</i>	35
Forensic Injury Biomechanics <i>Wilson C. Hayes, Mark S. Erickson, and Erik D. Power</i>	55
Genetic Engineering for Skeletal Regenerative Medicine <i>Charles A. Gersbach, Jennifer E. Phillips, and Andrés J. García</i>	87
The Structure and Function of the Endothelial Glycocalyx Layer <i>Seldon Weinbaum, John M. Tarbell, and Edward R. Damiano</i>	121
Fluid-Structure Interaction Analyses of Stented Abdominal Aortic Aneurysms <i>C. Kleinstreuer, Z. Li, and M.A. Farber</i>	169
Analysis of Time-Series Gene Expression Data: Methods, Challenges, and Opportunities <i>I.P. Androulakis, E. Yang, and R.R. Almon</i>	205
Interstitial Flow and Its Effects in Soft Tissues <i>Melody A. Swartz and Mark E. Fleury</i>	229
Nanotechnology Applications in Cancer <i>Shuming Nie, Yun Xing, Gloria J. Kim, and Jonathan W. Simons</i>	257
SNP Genotyping: Technologies and Biomedical Applications <i>Sobin Kim and Ashish Misra</i>	289
Current State of Imaging Protein-Protein Interactions In Vivo with Genetically Encoded Reporters <i>Victor Villalobos, Snehal Naik, and David Pivnicka-Worms</i>	321
Magnetic Resonance-Compatible Robotic and Mechatronics Systems for Image-Guided Interventions and Rehabilitation: A Review Study <i>Nikolaos V. Tsekos, Azadeh Khanicheh, Eftychios Christoforou, and Constantinos Mavroidis</i>	351

SQUID-Detected Magnetic Resonance Imaging in Microtesla Fields <i>John Clarke, Michael Hatridge, and Michael Mößle</i>	389
Ultrasound Microbubble Contrast Agents: Fundamentals and Application to Gene and Drug Delivery <i>Katherine Ferrara, Rachel Pollard, and Mark Borden</i>	415
Acoustic Detection of Coronary Artery Disease <i>John Semmlow and Ketaki Rabalkar</i>	449
Computational Anthropomorphic Models of the Human Anatomy: The Path to Realistic Monte Carlo Modeling in Radiological Sciences <i>Habib Zaidi and Xie George Xu</i>	471
Breast CT <i>Stephen J. Glick</i>	501
Noninvasive Human Brain Stimulation <i>Timothy Wagner, Antoni Valero-Cabre, and Alvaro Pascual-Leone</i>	527
Design of Health Care Technologies for the Developing World <i>Robert A. Malkin</i>	567

Indexes

Cumulative Index of Contributing Authors, Volumes 1–9	589
Cumulative Index of Chapter Titles, Volumes 1–9	593

Errata

An online log of corrections to *Annual Review of Biomedical Engineering* chapters (if any, 1977 to the present) may be found at <http://bioeng.annualreviews.org/>